TROPICAL LIFE SCIENCES RESEARCH

New Endiandric Acid from *Beilschmiedia lumutensis* and Their Molecular Docking Study as α-amylase and α-glucosidase Inhibitors

Authors:

Nur Amirah Saad, Muhammad Solehin Abd Ghani, Mohammad Tasyriq Che Omar, Mohd Azlan Nafiah, Unang Supratman, Desi Harneti, Cecile Apel, Marc Litaudon, Azeana Zahari, Khalijah Awang and Mohamad Nurul Azmi*

***Correspondence:** mnazmi@usm.my

Submitted: 13 November 2024; **Accepted:** 16 June 2025; **Early view:** 19 August 2025

To cite this article: Nur Amirah Saad, Muhammad Solehin Abd Ghani, Mohammad Tasyriq Che Omar, Mohd Azlan Nafiah, Unang Supratman, Desi Harneti, Cecile Apel, Marc Litaudon, Azeana Zahari, Khalijah Awang and Mohamad Nurul Azmi. (in press). New endiandric acid from *Beilschmiedia lumutensis* and their molecular docking study as α-amylase and α-glucosidase inhibitors. *Tropical Life Sciences Research.*

Highlights

- The isolation and purification of the bark of *Beilschmiedia lumutensis* isolate 3 new endiandric acids.
- The ethyl acetate crude of *Beilschmiedia lumutensis* showed the potential to inhibit α-amylase and α-glucosidase with IC_{50} values of 7.90 ± 1.00 µg/mL and 21.91 ± 3.93 µg/mL, respectively.
- Lumutensic acid C (**3**) showed the highest binding affinity and stability with both enzymes, with strong hydrogen bonding and hydrophobic interactions, compared to acarbose (control).
- This is the first report on the chemical constituents of *Beilschmiedia lumutensis*.

EARLY VIEW

New Endiandric Acid from *Beilschmiedia lumutensis* and Their Molecular Docking Study as α-amylase and α-glucosidase Inhibitors

[1]Nur Amirah Saad, [1]Muhammad Solehin Abd Ghani, [2]Mohammad Tasyriq Che Omar, [3]Mohd Azlan Nafiah, [4]Unang Supratman, [4]Desi Harneti, [5]Cecile Apel, [5]Marc Litaudon, [6]Azeana Zahari, [6]Khalijah Awang and [1]Mohamad Nurul Azmi*

[1]Natural Products and Synthesis Organic Research Laboratory (NPSO), School of Chemical Sciences, Universiti Sains Malaysia, 11800 Minden, Penang, Malaysia.
[2]Biological Section, School of Distance Education, Universiti Sains Malaysia, 11800 Minden, Pulau Pinang, Malaysia
[3]Department of Chemistry, Faculty of Science and Mathematics, Sultan Azlan Shah Campus, Universiti Pendidikan Sultan Idris, Proton City 35950, Perak Darul Ridzuan, Malaysia
[4]Department of Chemistry, Faculty of Mathematics and Natural Sciences, Universitas Padjadjaran, 45363 Jatinangor, Indonesia.
[5]Institut de Chimie des Substances Naturelles, CNRS, UPR 2301, Université Paris-Saclay, 91198 Gif-sur-Yvette, France
[6]Department of Chemistry, Faculty of Science, University of Malaya, 50603 Kuala Lumpur, Malaysia

***Corresponding author:** mnazmi@usm.my

Running head: New Endiandric Acid from *B. lumutensis*

Submitted: 13 November 2024; **Accepted:** 16 June 2025; **Early view:** 19 August 2025

To cite this article: Nur Amirah Saad, Muhammad Solehin Abd Ghani, Mohammad Tasyriq Che Omar, Mohd Azlan Nafiah, Unang Supratman, Desi Harneti, Cecile Apel, Marc Litaudon, [6]Azeana Zahari, Khalijah Awang and Mohamad Nurul Azmi (in press). New endiandric acid from *Beilschmiedia lumutensis* and their molecular docking study as α-amylase and α-glucosidase inhibitors. *Tropical Life Sciences Research.*

Abstract: A preliminary study showed that an ethyl acetate extract of the bark from *Beilschmiedia lumutensis* (Lauraceae family) exhibited promising inhibition activities against α-amylase and α-glucosidase by *in vitro* assays. Subsequently, this extract revealed three new cyclic polyketides endiandric acids, namely lumutensic acid A-C (**1**-**3**). Their structures were elucidated by 1D and 2D NMR, FT-IR, HRESIMS spectroscopic data analysis and by comparison with literature data. The molecular docking study showed that lumutensic acid C (**3**) showed the highest binding affinity and stability with both enzymes, with strong hydrogen bonding and hydrophobic interactions, outperfoming the standard drug acarbose. These findings suggest that compound **3** could be a promising candidate for anti-hyperglycemic therapeutic development, providing further insight into the potential of *B. lumutensis* as a source of bioactive compounds.

Keywords: Lauraceae; *Beilschmiedia lumutensis*; Cyclic polyketides; Endiandric acids; Molecular docking

INTRODUCTION

Beilschmiedia is one of the largest pantropical genera in Lauraceae family which about 287 species being recognised mainly in Southeast Asia and Africa (Nishida, 1999). In Southeast Asia, *Beilschmiedia* can be found in Vietnam, Myanmar, Thailand, Cambodia, Indonesia, Philippines, Malaysia and various island such as Sumatra and Java (Burkill, 1966). This genus is rich in source of pharmacologically active chemical constituents, so they have been widely used in medicinal field (Iwu, 1993). *Beilschmiedia lumutensis* (*B. lumutensis*) are trees 3 to 15 m tall endemic to Peninsular Malaysia and Cambodia and vegetate in lowland and hill forests at 150 m to 200 m altitude and sometimes on sandstone or near streams.

Endiandric acids, which possess a distinctive tetracyclic carbon skeleton formed with 11 or 13 carbon atoms including one or two double bonds and seven or eight sp^3 hybridised methines, are exclusively produced by the *Beilschmiedia* and *Endiandra* species. These cyclic polyketides of types A, B or B′ (Figure 1) have eight chiral centres and are generally isolated as a racemic mixture [αD] = 0° (Saad et al., 2022). This is a rather unusual observation for naturally occurring compounds resulting from both shikimate and acetate pathways (Lenta et al., 2015; Saad et al. 2022).

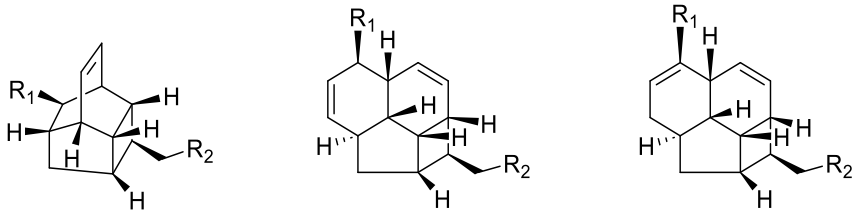

Endiandric acid type A Endiandric acid type B Endiandric acid type B'

Figure 1. Endiandric acids main skeleton.

Previous studies show that 14 species of the genus *Beilschmiedia* have been investigated, in which 55 of the isolated compounds have been identify as endiandric acids. The genus Beilschmiedia still holds considerable potential for exploration due to the unique architecture of its compounds (Lenta et al., 2015; Saad et al. 2022). In addition, previous studies showed that an ethyl acetate (EtOAc) extract of *B. lumutensis* bark exhibited inhibition activities against α-amylase and α-glucosidase with IC_{50} values of 7.90 ± 1.00 µg/mL and 21.91 ± 3.93 µg/mL, respectively (Tay et al., 2020). Based on this result and our previous study on various *Beilschmiedia* and *Endiandra* spp (Abu Bakar et al., 2020; Apel et al., 2014; Azmi et al., 2014; Azmi et al., 2016; Azmi et al., 2021; Saad et al., 2022; Tay et al., 2019), we decided to further explore the potential of the chemical constituents isolated from *B. lumutensis* to inhibit the two mentioned enzymes. In addition, molecular docking study was carried out to investigate the binding interactions of the isolated compounds with the active residues of α-amylase and α-glucosidase. This is the first report on the chemical constituents of this plant.

MATERIALS AND METHOD

General

The commercial chemicals and reagents used in the isolation and characterisation process of all the isolated compounds are as follows: hexane, AR grade (QRëC); ethyl acetate, AR grade (QRëC); methanol, AR grade (QRëC);dichloromethane, AR grade (QRëC); acetone, AR grade (QRëC); ethanol, AR grade (QRëC); formic acid (Merck), sulphuric acid (Merck); acetonitrile, HPLC grade (Merck); methanol, HPLC grade (Merck); chloroform-d_1 for NMR (Merck); methanol-d_4 for NMR (Merck); silica gel 60 for column chromatography, 0.040 – 0.063 mm and 0.063 –

0.200 mm (Merck); TLC silica gel 60 F_{254}, aluminium sheets, 20 cm × 20 cm (Merck). All solvents were used without further purification, unless otherwise stated.

Flash chromatographic techniques under controlled pressure were used with silica gel 60 (0.06-0.2 mm) and subsequent purification with 230-400 and 70-230 silica gel mesh as well as pre-coated TLC silica 60 gel F_{254} 20 x 20 cm on aluminium sheet (Merck). The TLC sheet were observed under 254 nm UV lamp while the vanillin-sulfuric acid reagent and heating gun were used for further visualisation. High-performance liquid chromatography (HPLC) was used for further purification process by using the JAI Recycling HPLC with model no. of LC-9130 NEXT. It was a semi preparative HPLC, smart and compact instrument since all-in-one body. This instrument has panel to control the injector, detector, pump and fraction collector from the computer or LCD touch screen panel. UV detector was used to detect four selected wavelengths from 200 to 800 nm. In this research, it favoured wavelength at 210 nm. 10 mg of the selected fractions with two or three spots on TLC were dissolved in 1 mL MeOH. Then, it was eluted with a mixture of MeOH: H_2O with ratio of 60:40 in the presence of 0.1% formic acid as a buffer. Prior to analysis, all solvents were filtered with a nylon membrane filter that has a pore size of 0.45 µm. The fractions were eluted at a flow rate of 4.0 mL min^{-1}. Next, the NMR spectra were obtained by using a Bruker Advance 500 (500 MHz for ^{1}H NMR, 125 MHz for ^{13}C NMR) spectrometer system. Data were analysed via TopSpin 3.6.3 software package. Spectra were referenced to TMS or residual solvent (chloroform-d_1 ($CDCl_3$) = 7.26 ppm in ^{1}H NMR and 77.2 ppm in ^{13}C NMR; methanol-d_4 (CD_3OD) = 3.31 ppm, 4.87 ppm in ^{1}H NMR and 49.3 ppm in ^{13}C NMR). ^{1}H NMR spectroscopic data is reported as follows: chemical shift (relative integral, multiplicity [s – singlet, d – doublet, dd – doublet of doublets, dt – doublet of triplets, t – triplet, m – multiplet] spin – spin coupling constant (*J* in Hertz, Hz). The HRESIMS were carried on a Thermoquest TLM Deca ion-trap mass spectrometer and Agilent 1290 Infinity Ultra-Performance Liquid Chromatography-Tandem Mass Spectrometer (UHPLC-MS/MS) by using direct infusion. Infrared (IR) spectra of the compounds were obtained using Perkin Elmer 2000 FT-IR at the School of Chemical Sciences, USM. All samples were analysed in the range of 4000 – 600 cm^{-1} wavelengths to determine the functional group. The result formed a spectrum designated as% transmittance versus wavenumber (cm^{-1}).

Plant Material

The bark of *Beilschmiedia lumutensis* (*B. lumutensis*) was collected in Machang, Kelantan, Malaysia in July 2006. This species was identified by Teo L. E., a botanist from Department of

Chemistry, Faculty of Science, University of Malaya. A voucher specimen (KL5269B) has been deposited at the Herbarium of the Department of Chemistry, Faculty of Science, University of Malaya, Kuala Lumpur, Malaysia for future reference.

Extraction and Isolation of Compounds

The air-dried bark of *B. lumutensis* (1.5 kg) were sliced, ground into small pieces and extracted with EtOAc (3×1.5 L) followed by MeOH (3×1.5 L) at room temperature using maceration process. The solvents were evaporated under reduced pressure at 40°C to give 61.4 g (4.1%) of EtOAc and 69.2 g (4.4%) of MeOH extracts, respectively. The EtOAc crude extract (61.0 g) was subjected to CC (silica gel, 0.063 – 0.200 mm, *n*-hexane:EtOAc step gradient) to afford 10 fractions (BL_F1-F10). Selected fractions were subjected to semi-preparative recycling HPLC, using isocratic method with 60% MeOH:40% H_20 + 0.1% formic acid to give desired compounds. Fractions BL_F2 and BL_F3 were combined and further fractionated by using CC (silica gel, 0.040 – 0.063 mm; *n*-hexane:EtOAc step gradient) to obtain 12 subfractions. BL_F2.1 (0.21 g) was then separated by using recycling HPLC (60% MeOH:40% H_20 + 0.1% formic acid) to afford lumutensic acid A (**1**, 1.8 mg). Next, BL_F2.3 (0.44 g) was further fractionated to give lumutensic acid B (**2**, 1.1 mg). BL_F2.5 weighed 0.58 g underwent further separation process by CC and yielded lumutensic acid C (**3**, 3.6 mg). The structure of isolated compounds were determined by spectroscopic analysis (See supporting information).

Lumutensic acid A (**1**): White solid; Yield: 1.8 mg (0.013%); FT-IR (ATR) V_{max} cm^{-1}: 3421 cm^{-1} (hydroxyl group), 2922 cm^{-1} (C–H stretching symmetric CH_2), 2854 cm^{-1} (C–H stretching asymmetric CH_2) and 1705 cm^{-1} (carbonyl group); HRESIMS: *m/z* 316.1920 $[M-H]^-$ (calc. mass 316.2402); ^{1}H-NMR (500 MHz, MeOH-D4): See Table 1; ^{13}C-NMR (125 MHz, MeOH-D_4): See Table 1

Lumutensic acid B (**2**): White solid; Yield: 1.1 mg (0.008%); HRESIMS: *m/z* 387.1438 $[M+H]^+$ (calc. mass 387.3263); ^{1}H-NMR (500 MHz, $CDCl_3$): See Table 1; ^{13}C-NMR (125 MHz $CDCl_3$): See Table 1

Lumutensic acid C (**3**): Yellowish; Yield: 3.6 mg (0.025%); HRESIMS: *m/z* 434.3249 (calc. mass 434.2457); ^{1}H-NMR (500 MHz, $CDCl_3$): See Table 1; ^{13}C-NMR (125 MHz $CDCl_3$): See Table 1

Molecular Docking

The molecular docking studies were performed according to the method described by the previous publications with some modifications (Mahdi et al., 2024(a); Mahdi et al., 2024(b); Mohamad et al., 2021; Radzuan et al., 2024; Saad et al., 2022). Briefly, for the *in silico* assessment of anti-hyperglycemic, the receptors from the Protein Data Bank (PDB) database (https://www.rcsb.org/) were used, including the crystallographic structure of human pancreatic α-amylase in complex with nitrite and acarbose (PDB ID: 2QV4), which was resolved to a high resolution of 1.97 Å for α-amylase inhibition studies. For the α-glucosidase inhibition studies, the crystal of human intestinal C-terminal maltase-glucoamylase (ctMGAM) in complex with acarbose (PDB ID: 3TOP) was used with a resolution of 2.88 Å for molecular docking analysis. These two protein receptors were prepared using the DockPrep tools in UCSF Chimera (Regents of University of California, CA, USA) graphical user interface (GUI) (Pettersen et al., 2004) by removing water molecules, unrelated heteroatoms and co-crystal complexes. Protein preparation continued with the addition of polar hydrogens, the merger of non-polar hydrogens, and the addition of solvation parameters and Gasteiger charges, which were saved in .pdbqt format. In addition, the 3D structure of the compounds was sketched using ChemDraw Professional 23.0 (Revvity Signals Software, MA, USA), followed by ligand preparation and energy minimisation using the MM2 force field in the Chem3D tools, which were then saved as .pdb. The grid boxes were placed around co-crystallised ligand, which was acarbose for both α-amylase α-glucosidase. Specifically, docking for α-amylase was conducted using a grid box parameter centred at coordinates 14.5, 48.5 and 29.0 along the X, Y and Z axes, respectively, with a spacing of 0.375 Å and a grid size of 25 × 25 × 25 Å (X, Y and Z) to ensure comprehensive coverage of the active site of the enzyme. For α-glucosidase, the centre of the grid box was set to -30.6, 35.6 and 26.5 along the X, Y and Z axes, with a spacing of 0.375 Å and a grid box size of 30 × 30 × 30 Å (X, Y and Z). Computational docking simulations were carried out using the binding analysis/docking module of UCSF Chimera-AutoDock Vina (Eberhardt et al., 2021; Trott O, and Olson A J, 2010). Ligand-receptor docking results from AutoDock Vina were further analysed and visualised in 2D and 3D conformations through BIOVIA Discovery Studio Visualizer 2024 Client (Dassault Systemes, CA, USA).

RESULTS AND DISCUSSSION

Phytochemical studies identified three compounds classified as endiandric acid derivatives: two endiandric acid type A compounds, lumutensic acid A (**1**) and lumutensic acid B (**2**), and one endiandric acid type B compound, lumutensic acid C (**3**). All spectroscopic data and spectra are provided in this section.

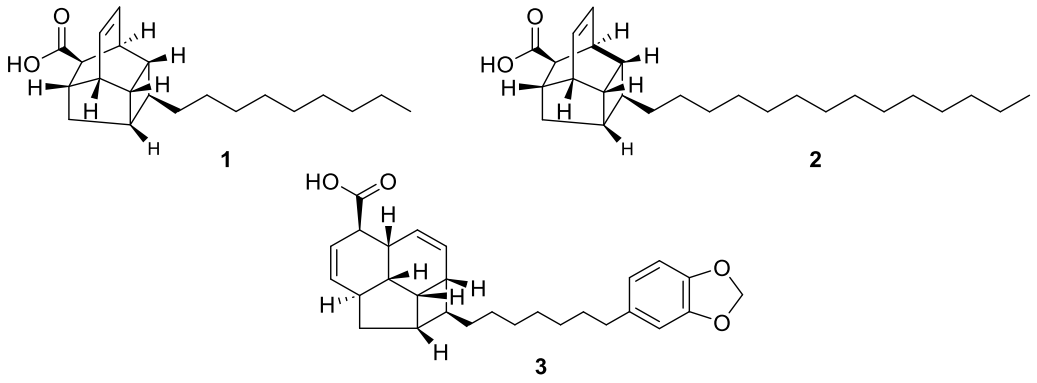

Figure 1. The structures of endiandric acids **1**-**3** isolated from the bark of *B. lumutensis*

Compound **1** was obtained as a white solid. It was classified as endiandric acid type A with molecular formula of $C_{21}H_{32}O_2$, assignable on the basis of HRMS data by a molecular ion peak at $[M+H]^+$ at m/z 316.1920 (calcd. for 316.2402) with 6 degrees of unsaturation. The IR showed absorption band at λ_{max}; 3421 cm^{-1}, 2922 cm^{-1}, 2854 cm^{-1} and 1705 cm^{-1} indicating the presence of hydroxyl group, C–H stretching (sp^3 hybridization) for symmetric CH_2, C–H stretching (sp^3 hybridization) for asymmetric CH_2 and carbonyl group, respectively. Based on ^1H NMR spectrum (Table 1), the unique characteristics of endiandric acid type A revealed at δ_H 6.14 (J = 7.1 Hz) and δ_H 6.24 (J = 7.3 Hz). Both peaks appeared as triplet which representing the *cis* double bond at H-10 and H-11. Next, a triplet signal at δ_H 0.91 (J = 6.6 Hz) confirmed the presence of terminal methyl. An alkyl chain can be affirmed by a broad peak resonated at δ_H 1.32. In addition, the ^{13}C NMR and DEPT135 spectra showed twenty-one signals: ten methines, nine methylenes, one methyl and one quaternary carbon (Table 1). The core structure which known as 'cage like structure' were represented by eleven skeletal signals resonated at δ_C 43.5 (C-1), 41.6 (C-2), 40.9 (C-3), 41.2 (C-4), 41.9 (C-5), 39.9 (C-6), 40.6 (C-7), 52.0 (C-8), 36.9 (C-9), 131.5 (C-10), 133.9 (C-11). Eight methylenes carbon resonated between δ_C 23.82 to 33.17 confirmed the alkyl chain.

Since the proton signals of alkyl group was broad, the positions of C1' to C8' were determined by the shielding and deshielding effects in carbon spectrum. C1' was more deshielded than C2' due to its position which was more adjacent to the electron withdrawing group. The further the alkyl carbon from the functional group, the lower the chemical shift. The linkage between the core structure was validated by the ^{1}H-^{1}H COSY spectrum (Figure 2). The correlations between H-1/H-2, H-2/H-5, H-5/H-6β, H-6β/H-7, H-7/H-1 and H-8/H-9, H-9/H-3, H-3/H-2, H-2/H-1, H-1/H-7 and H-7/H-8 portrayed the existence of a cyclopentane (C1-C2-C5-C6-C7) and cyclohexane (C9-C3-C2-C1-C7-C8). In addition, a cyclobutene (C2-C3-C4-C5) and a six membered ring (C10-C11-C1-C2-C3-C9) were demonstrated by the correlations of H-10/H-11, H-11/H-1, H-1/H-2, H-2/H-3, H-3/H-9, H-9/H-10 and H-2/H-3, H-3/H-4, H-4/H-5 and H-5/H-2, respectively. The existence of carboxylic acid group was affirmed by the cross peak showed in HMBC. The correlations between H-7/C=O, H-8/C=O indicate that the position of carboxylic was bonded to C-8. Compound **1** was deduced as (1*S*,2*R*,3*R*,4*S*,5*S*,7*S*,8*R*,9*S*)-4-nonyltetracyclo[5.4.0.02,5.03,9]undec-10-ene-8-carboxylic acid also known as lumutensic acid A and it was a new endiandric acid type A.

Compound **2** was obtained as white solid. It was classified as endiandric acid type A. The HRMS spectrum of compound **2** revealed a molecular ion peak in a positive mode $[M+H]^{+}$ at m/z 387.1438 (calc. mass 387.3263) corresponding with molecular formula of $C_{26}H_{42}O_2$ and 6 degrees of unsaturation. The ^{1}H NMR spectrum of compound **2** revealed the key features of 'cage like structure' with overlapping two triplets signal at δ_H 6.23, corresponding to *cis* olefinic protons at C-10 and C-11 (Table 1). Similar to compound **1**, terminal methyl was confirmed by the presence of triplet peak resonated at δ_H 0.93. A broad peak at δ_H 1.25 proved the occurrence of a long alkyl chain representing nine protons at H-4'- H-12'. Based on ^{13}C and DEPT135 spectra, there were twenty-six signals with ten methines, fourteen methylenes, one methyl and one quaternary carbon (Table 1). The carboxylic acid was presented by quaternary signal resonated at δ_C 177.5. Ten methines resonated at δ_C 42.1 (C-1), 40.3 (C-2), 39.7 (C-3), 39.8 (C-4), 40.5 (C-5), 38.6 (C-7), 48.9 (C-8), 35.3 (C-9), 131.6 (C-10), 132.1 (C-11) and a methylene resonated at δ_C 38.7 (C-6). A long alkyl chain for compound **2** were confirmed by carbon signal in the range of δ_C 14.3 to 36.5. Carbon at C-1' had higher chemical shift than neighbouring C-2', C-3' and so forth because of the deshielding effects. The ^{1}H-^{1}H COSY and HMBC correlation helped to determine the positions of the carbon and proton in this compound (Figure 2). The cross peaks between H-8/C=O, H-7/C=O, H-8/C-O approved the position of carboxylic acid bonded to C-8. The neighbouring protons in the main skeleton were confirmed by the corelations of H-9/H-10, H-11/H-1, H-9/H-8, H-9/H-3, H-7/H-6, H-2/H-3, H-6/H-5, H-5/H-4, H-7/H-1, H-2/H-1 and H-9/H-3. Finally, with the aid from 1D and 2D spectroscopic data and published data, compound **2** was confirmed to be

(1*S*,2*R*,3*R*,4*S*,5*S*,7*S*,8*R*,9*S*)-4-tetradecyltetracyclo[5.4.0.02,5.03,9]undec-10-ene-8-carboxylic acid known as lumutensic acid B and it was also a new endiandric acid type A.

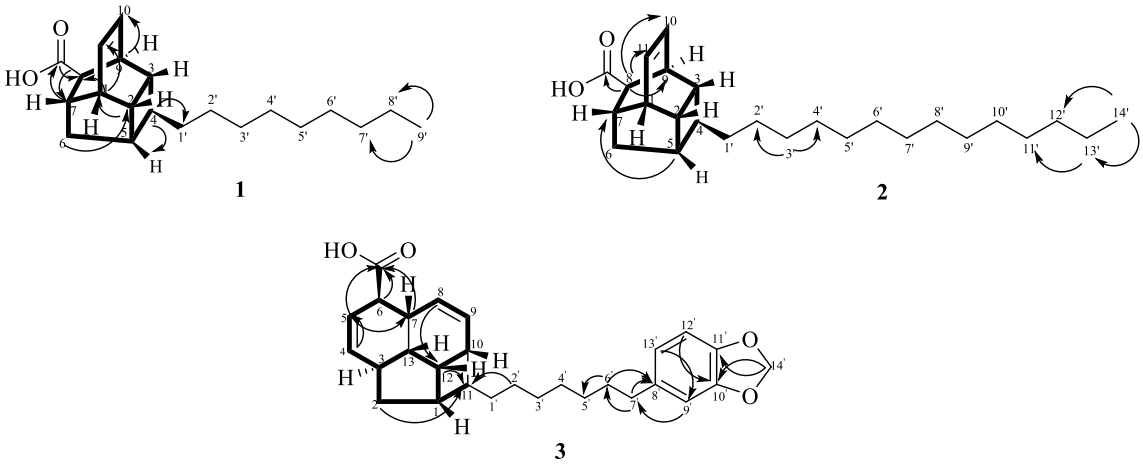

Figure 2. ^{1}H-^{1}H COSY (bold) and HMBC (^{1}H→^{13}C) correlations of endiandric acids **1**-**3**.

Compound **3** was obtained as yellowish oil. It was classified as endiandric acid type B with molecular formula of $C_{28}H_{34}O_4$ was determined by HRMS analysis in a positive mode $[M+H]^+$ with molecular ion peak at m/z 434.3249 (calc. mass 434.2457), consistent with 12 degrees of unsaturation. The ^{1}H NMR spectrum revealed the unique characteristics features of endiandric acid type B with *cis* double bonds at δ_H 6.22 (dt, *J* = 9.7, 2.5 Hz), 5.74 (dt, *J* = 9.7, 2.9 Hz), 5.46 (dt, *J* = 3.7, 10.1 Hz) and 5.64 (br dt, *J* = 3.7, 10.1 Hz) assignable to C-4, C-5, C-8 and C-9 (Table 1). Next, the presence of a benzene ring can be assured by three proton signals resonated at δ_H 6.66 (d, *J* = 1.0 Hz) 6.71 (d, *J* = 7.8 Hz) and 6.61 (dd, *J* = 7.8, 1.0 Hz) representing C-9', C-12' and C-13', respectively. A singlet peak resonated at δ_H 5.91 portrayed the presence of methylenedioxyphenyl group. Meanwhile, the ^{13}C NMR and DEPT135 spectra showed the presence of sixteen methines and nine methylenes (Table 1). Four *cis* form alkene carbon signals resonated at δ_C 134.7 (C-4), 124.1 (C-5), 129.7 (C-8) and 129.8 (C-9) confirmed the key features for endiandric acid type B. One out of four quaternary carbon revealed by ^{13}C NMR illustrated the presence of carboxylic acid, COOH group which resonated at δ_C 179.3. Three methine carbon resonated at δ_C 109.0 (C-9'), 108.20 (C-12') and 121.20 (C-13') represents the aromatic ring while one methylene carbon resonated at δ_C 100.9 showed the presence of methylenedioxyphenyl substituent. The 2D NMR spectra (HSQC, HMBC and COSY) were further studied to confirm the structure (Figure 2). The HMBC correlations revealed the position of COOH group at C-6 through

the cross peaks, of H6/C=O, H-5/C=O and H-7/C=O. Besides, the methylenedioxyphenyl moiety attached to C-8' was confirmed by the HMBC correlation of H-13'/C-7', H-9'/C-7', H-6'/C-8, H-7'/C-6'and H-7'/C-8'. COSY correlation as shown in Figure 2 with correlations at H-12/H-1, H-3/H-1, H-5/H-6, H-9/H-7, H-4/H-5, H-4/H-6 and H-4/H-3. On a final note, on comparison with spectroscopic data and literature, compound **2** was elucidated as (1*S*,2*S*,3*R*,6*R*,7*R*,10*S*,11*S*,12*S*)-2-(1,3-benzodioxol-5-ylheptyl)tetracyclo[8.2.1.03,12.06,11]trideca-4,8-diene-7-carboxylic acid also known as lumutensic acid C and this is a new endiandric acid type B found in *B. lumutensis*.

The EtOAc extract was evaluated to α-amylase and α-glucosidase assays and it shows a good inhibition with IC_{50} values 7.90 ± 1.00 µg/mL and 21.91 ± 3.93 µg/mL, respectively (Tay et al., 2020). Due to limited amount of compounds, we decided to perform a molecular docking study to understand the free binding energy and interaction modes between the residues in the active site of the enzymes and compounds **1**-**3**.

Table 1. ^{1}H (500 MHz) and ^{13}C (125 MHz) NMR data of compounds **1** (CD_3OD), **2** and **3** ($CDCl_3$).

Position	Compound 1		Compound 2		Compound 3	
	δ_H (*J* in Hz)	δ_C	δ_H (*J* in Hz)	δ_C	δ_H (*J* in Hz)	δ_C
1	2.65 m	43.5	2.69 m	42.1	2.27 m	41.4
2	2.34 m	41.6	2.36 t (7.5)	40.3	1.33 dd (5.8, 12.8)	34.9
					1.58 m (5.3, 11.8)	
3	1.73 m	40.9	1.63 m	39.7	2.56 m	37.1
4	1.60 m	41.2	1.63 m	39.8	6.22 dt (9.7, 2.5)	134.7
5	2.23 m	41.9	2.22 br, d (6.3)	40.5	5.74 dt (9.7, 2.9)	124.1
6	1.58 m	39.9	1.55 d (12.7)	38.7	3.03 m	49.31
	1.91 m		1.90 m			
7	2.56 m	40.6	2.55 m	38.6	3.00 m	33.05
8	2.74 d (3.2)	52.0	2.88 d (3.6)	48.6	5.46 dt (3.7, 10.1)	129.7
9	2.99 m	36.9	3.03 m	35.3	5.64 br, dt (3.7,	129.8
					10.1)	
10	6.14 t (7.1)	131.5	6.23 m	131.6	2.26 m	35.1
11	6.24 t (7.3)	133.9	6.23 m	132.1	1.45 m	46.1
12	-	-	-	-	2.65 q (7.8)	33.2
13	-	-	-	-	1.72 m	42.2
1'	1.27 br	33.2	1.49 m	36.5	1.47 m	37.3

2'	1.32 m	30.9	2.35 m	33.7	1.22 m	27.1
3'	1.32 m	30.9	1.62 m	24.9	1.27 m	29.6
4'	1.32 m	30.8	1.25 m	29.9	1.27 m	29.3
5'	1.32 m	30.8	1.25 m	29.9	1.27 m	29.7
6'	1.32 m	30.5	1.25 m	29.8	1.56 m	31.9
7'	1.32 m	28.5	1.25 m	29.7	2.51 t (7.6)	35.9
8'	1.31 m	23.8	1.25 m	29.6	-	136.9
9'	0.91 t (6.6)	14.5	1.25 t (6.6)	29.5	6.66 d (1.0)	109.0
10'	-	-	1.25 m	29.3	-	147.6
11'	-	-	1.25 m	27.5	-	145.5
12'	-	-	1.25 m	32.1	6.71 d (7.8)	108.2
13'	-	-	1.31 m	22.9	6.61 dd (7.8, 1.0)	121.2
14'	-	-	0.94 t (6.9)	14.3	5.91 s	100.9
C=O	-	181.7	-	179.5	-	179.4

Molecular docking simulations were conducted to calculate the theoretical binding energy and to simulate the binding interactions of the isolated compounds **1**-**3** in the hyperglycemic enzymes of α-amylase (PDB ID: 2QV4) and α-glucosidase (PDB ID: 3TOP). α-Amylase is a key enzyme in the breakdown of carbohydrates into glucose. By inhibiting this enzyme, the rate of glucose uptake can be reduced, which has a positive effect on the control of blood sugar levels in diabetics (Maurus et al., 2008). Besides, the MGAM protein is a type of α-glucosidase enzyme that is crucial in the final steps of carbohydrate digestion by breaking down starch into glucose. The C-terminal MGAM (ctMGAM) was selected as the docking protein for α-glucosidase as it has been reported to be favoured over the N-terminal when inhibited with acarbose (Phongphane et al., 2023). Of note, inhibition of this enzyme may help to control postprandial blood glucose levels, which is essential for the control of diabetes (Ren et al., 2011).

Before initiating the molecular docking simulation, the docking parameters were validated by redocking the co-crystallised (native) ligands, namely acarbose, to the active site of these enzymes. The calculated root mean square deviation (RMSD) between the native and redocked ligands (Figure 3) yielded values of 0.883 Å (α-amylase) and 0.465 Å (α-glucosidase), which are well below the acceptable threshold of 2.00 Å, indicating that the docking procedure is valid and can be used for compound docking (Bell, E.W and Zhang, Y., 2019; Zheng et al., 2022). Additionally, even with its bulky planar structure, acarbose forms stable complexes by directly interacting with the catalytic amino acids in the active sites of α-amylase and α-glucosidase, causing their 3D structures to adopt guided conformations similar to synthetic molecules (Şahin

et al., 2023). Hence, the binding energies and inhibition constant of α-amylase and α-glucosidase with the target compounds and the docking controls are listed in Table 2, while the type of the binding interactions is detailed in Tables 3 and 4. As shown in Table 2, the negative binding energy and low inhibition constant of all target compounds indicate that the interactions with the receptor of the enzymes are thermodynamically favourable with an appreciable binding energy (Basir et al., 2024).

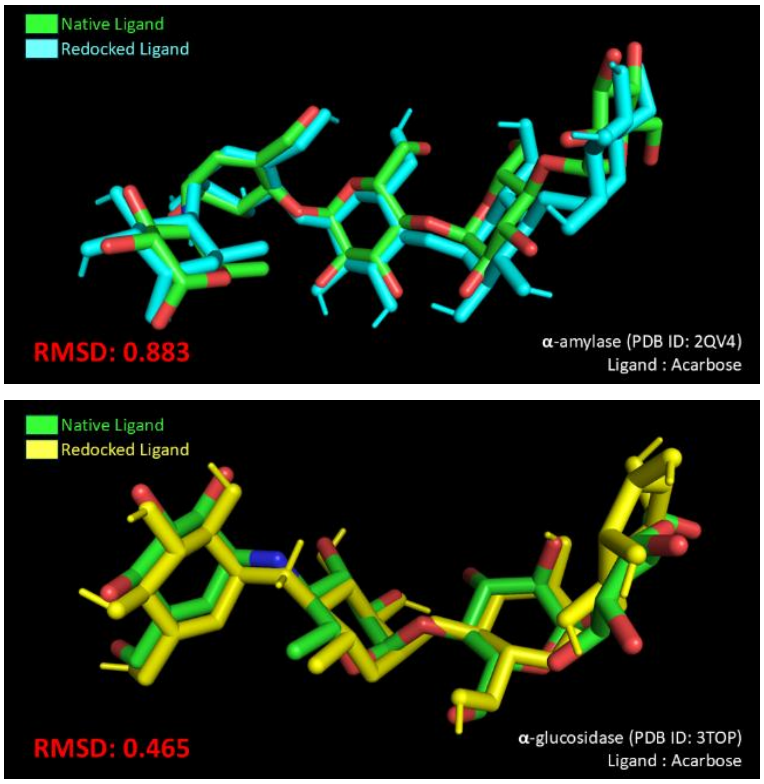

Figure 3. Root mean square deviation (RMSD) for α-amylase (left) and α-glucosidase (right).

Table 2. *In silico* binding energy of compounds **1**-**3** and acarbose on α-amylase (2QV4) and α-glucosidase (3TOP).

Protein	Compound	Binding energy, ΔG (kcal/mol)	Inhibition constant, K_i [K = exp(ΔG/RT)]
α-amylase (PDB ID: 2QV4)	**1**	-6.964 ± 0.016	7.757×10^{-6}
	2	-6.718 ± 0.074	1.175×10^{-5}
	3	-9.070 ± 0.128	2.209×10^{-7}
	Acarbose (Docking control)	-9.228 ± 0.010	1.692×10^{-7}
α-glucosidase (PDB ID: 3TOP)	**1**	-7.553 ± 0.107	2.867×10^{-6}
	2	-7.298 ± 0.062	4.412×10^{-6}
	3	-9.275 ± 0.019	1.563×10^{-7}
	α-Acarbose (Docking control)	-7.488 ± 0.129	3.200×10^{-6}

± Standard deviation for n = 3 experiments

In the docking evaluation of α-amylase, all isolated compounds exhibited a higher binding energy and lower binding affinity with the enzyme, ranging from -9.070 to -6.718 kcal/mol, compared to acarbose (docking control, standard drug) at -9.228 ± 0.010 kcal/mol. The molecular docking investigation of compound **1** revealed several interesting interactions with the binding site residues (Figure 4a), with the ΔG of -6.964 ± 0.016 kcal/mol and K_i of 7.757×10^{-6}. The residues of ARG195, GLU233 and ASP300 engaged in the conventional hydrogen bonds with the -OH moiety, while HIS299 formed a similar hydrogen bond with the carbonyl group of **1**, which stabilised the complex. In addition, two π-alkyl interactions were established between $-CH_2$ moieties and the residues of TRP58 and TRP59. The cyclohexyl rings of **1** interact with LEU162 and ALA198 through alkyl interactions, whereas another $-CH_2$ interacts with LEU165 through similar interactions.

In compound **2** (ΔG of -6.718 ± 0.074 kcal/mol; K_i of 1.175×10^{-5}), the -C=O and -OH groups of this ligand formed conventional hydrogen bonds with HIS299 and ASP300, respectively, which contributes to the stabilisation of the ligand within the binding site of the enzyme (Figure 4b). Moreover, the side chains of residues TRP58, TRP59 and HIS305 interact with the $-CH_2$ hydrophobic regions of the ligand through π-alkyl interactions. Additionally, the alkyl side chain of LEU162, LEU165 and ALA198 interact with the alkyl groups of the ligand consisting of $-CH_2$, $-CH_3$

and the cyclohexyl ring through alkyl interactions, enhancing the hydrophobic interactions, which further contributed to the overall binding energy.

Compound **3** is the most stable docked complex with the highest binding affinity among the isolated compounds, with ΔG of -9.070 ± 0.128 kcal/mol and K_i of 2.209 × 10^{-7}. It exhibited two conventional hydrogen bonds. The first is the oxygen of the methylenedioxyl with the amino group of GLN63 and the second is the -OH of the ligand with the ASP300 residue. Besides, the -CH_2 of the methylenedioxyl participated in a carbon-hydrogen bond with the -C=O of ASP300, which drove the binding process. The π-alkyl interactions between TRP58, TYR62 and LEU165 with the alkyl segment of -CH_2 and the phenyl moieties of the ligand further stabilised the complex, while an alkyl interaction occurred between -CH_2 of **3** and LEU162 of the α-amylase enzyme (Figure 4c).

Table 3. The key interactions of the compounds **1**-**3** and acarbose with the amino acids of α-amylase (2QV4).

Protein	Compound	Residue	Moiety	Types of interaction
α-amylase (PDB ID: 2QV4)	**1**	TRP58	-CH_2	π-Alkyl
		TRP59	-CH_2	π-Alkyl
		LEU162	Ring (Cyclohexyl)	Alkyl
		LEU165	-CH_2	Alkyl
		ARG195	-OH	Conventional H-bond (1.99 Å)
		ALA198	Ring (Cyclohexyl)	Alkyl
		GLU233	-OH	Conventional H-bond (2.40 Å)
		HIS299	-C=O	Conventional H-bond (2.33 Å)
		ASP300	-OH	Conventional H-bond (2.59 Å)
	2	TRP58	-CH_2	π-Alkyl
		TRP59	-CH_2	π-Alkyl
			-CH_2	π-Alkyl
		LEU162	-CH_2	Alkyl
			Ring (Cyclohexyl)	Alkyl
		LEU165	-CH_2	Alkyl
			-CH_3	Alkyl

	ALA198	Ring (Cyclohexyl)	Alkyl
	HIS299	-C=O	Conventional H-bond (2.63 Å)
	ASP300	-OH	Conventional H-bond (2.53 Å)
	HIS305	$-CH_2$	π-Alkyl
3	TRP58	$-CH_2$	π-Alkyl
	TYR62	$-CH_2$	π-Alkyl
	GLN63	-O (Methylenedioxyl)	Conventional H-bond (2.63 Å)
	LEU162	$-CH_2$	Alkyl
	THR163	$-CH_2$ (Methylenedioxyl)	Carbon H-bond
	LEU165	Phenyl	π-Alkyl
	ASP300	-OH	Conventional H-bond (2.27 Å)
Acarbose (Docking control)	TYR62	-OH	Conventional H-bond (2.86 Å)
		-OH	Conventional H-bond (2.75 Å)
		-OH	Carbon H-bond
	HIS101	-O	Conventional H-bond (2.69 Å)
	ALA106	-O	Conventional H-bond (2.14 Å)
		-O	Conventional H-bond (2.49 Å)
	VAL107	-O	Conventional H-bond (2.53 Å)
	THR163	-OH	Conventional H-bond (2.60 Å)
		-CH	Carbon H-bond
	ALA198	-O	Carbon H-bond
	GLU233	-CH	Carbon H-bond
	HIS305	-OH	Conventional H-bond (2.84 Å)

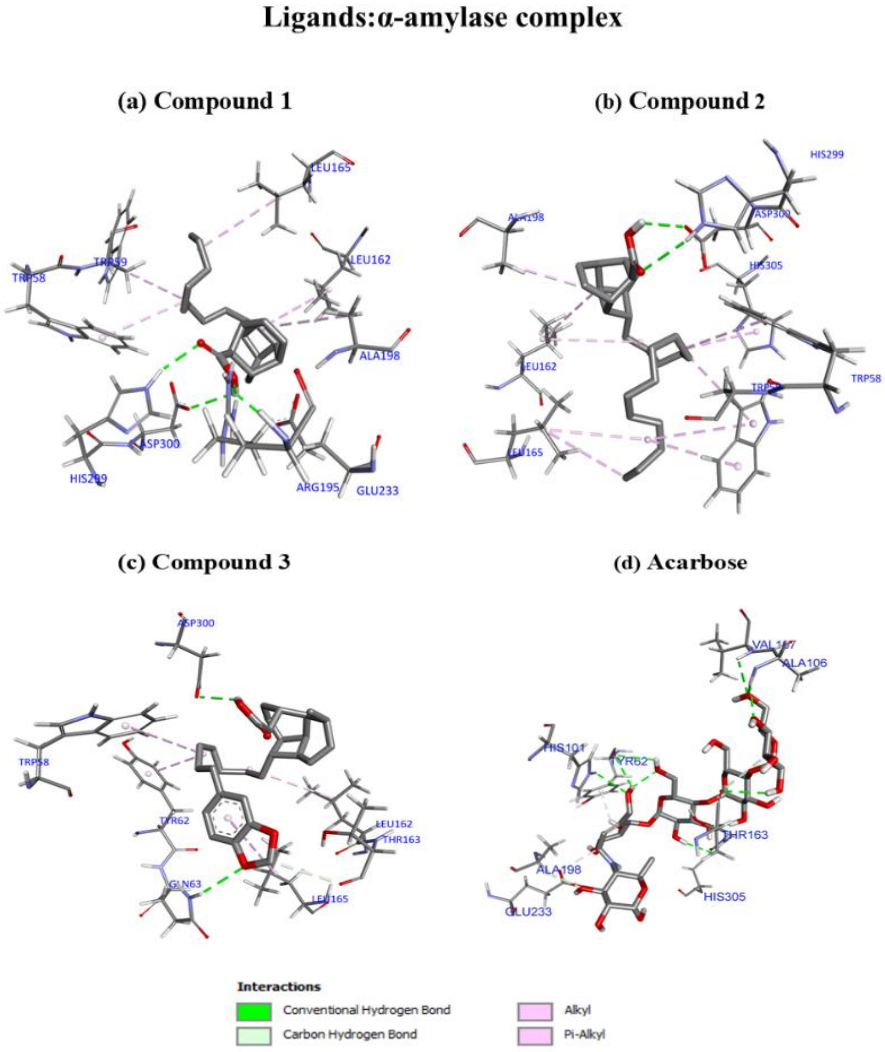

Figure 4. The three-dimensional binding modes of compounds **1**-**3** and acarbose are presented at the active site of α-amylase (2QV4).

Upon molecular docking of the α-glucosidase enzyme, all isolated compounds displayed comparable binding energy (in the range of -9.275 to -7.298 kcal/mol) as the acarbose control (-7.488 ± 0.129 kcal/mol). Of the three compounds analysed, compound **3** had the highest binding energy, followed by **1**. Compound **1** (ΔG of -7.553 ± 0.107; K_i of 2.867 × 10^{-6}) unveiled several interactions with the residues of the α-glucosidase binding site, such as a conventional hydrogen bonding interaction between the -OH group of **1** and the carboxyl groups of ASP1157 and ASP1526, and a carbon-hydrogen bonding interaction between -C=O of **1** and the PRO1159

residue. Further, the π-system of the pyrrole ring in the indole group of TRP1369 and the cyclohexyl ring of **1** showed a π-sigma interaction, which increases the binding intercalation strength. Meanwhile, eight other hydrophobic π-alkyl interactions occurred between the cyclohexyl ring and the -CH_2 moieties of the compound with TYR1251, TRP1355, TRP1369 and PHE1559, as shown in Figure 5a.

In compound **2** (ΔG of -7.298 ± 0.062; K_i of 4.412 × 10^{-6}), conventional hydrogen bonding were observed between the hydrogen atoms of the -OH group and the carboxyl of ASP1157 and ASP1526, while the -C=O in **2** interacts with the side chain of PRO1159 via a carbon hydrogen bond (Figure 5b). Interestingly, a π-sigma interaction formed between the -CH_2 group and the phenyl ring of the TYR1251 residue, which further stabilised the docked complex. In addition, the -CH_2 units in **2** also formed another hydrophobic interaction via alkyl and π-alkyl with the enzyme residues of ILE1280, TYR1251, TRP1355, ASP1526, PHE1559 and PHE1560. Finally, two π-alkyl interactions occurred between the TRP1369 residue and the cyclopentyl and cyclohexyl ring structure of **2**. Remarkably, compound **3** is the most promising compound in the *in silico* α-glucosidase evaluation with a good binding energy of -9.275 ± 0.019 kcal/mol and K_i of 1.563 × 10^{-7} (Figure 5c). This compound exhibited four conventional hydrogen bonds, the first two between the oxygen of -C=O with LYS1460 and two more between the oxygen of the methylenedioxyl group with ARG1510 and HIS1584. The next prominent interactions involved in this docked complex intercalation was π-π T-shaped between the phenyl group in **3** and the π-system of phenyl in residues TYR1251 and PHE1559, which contributed to the total binding energy. With the -CH_2 group, four π-alkyl interactions were formed with TYR1251, TRP1355 and TRP1369. Another π-alkyl interaction was observed between the cyclohexyl ring of **3** with the protein residue PHE1560 on the phenyl ring.

Table 4. The key interactions of the compounds **1**-**3** and acarbose with the amino acids of α-glucosidase (3TOP).

Protein	Compound	Residue	Moiety	Types of interaction
α-glucosidase (PDB ID: 3TOP)	**1**	ASP1157	-O<u>H</u>	Conventional H-bond (2.07 Å)
		PRO1159	-C=<u>O</u>	Carbon H-bond
		TYR1251	-CH_2	π-Alkyl
			-CH_2	π-Alkyl
		TRP1355	-CH_2	π-Alkyl

		Ring (Cyclohexyl)	π-Alkyl
	TRP1369	Ring (Cyclopentyl)	π-Sigma
		Ring (Cyclohexyl)	π-Alkyl
	PHE1427	Ring (Cyclohexyl)	π-Alkyl
	ASP1526	-O<u>H</u>	Conventional H-bond (2.53 Å)
	PHE1559	$-CH_2$	π-Alkyl
		$-CH_2$	π-Alkyl
2	ASP1157	-O<u>H</u>	Conventional H-bond (2.01 Å)
	PRO1159	-C=<u>O</u>	Carbon H-bond
	TYR1251	$-CH_2$	π-Sigma
		$-CH_2$	π-Alkyl
	ILE1280	$-CH_2$	Alkyl
	TRP1355	$-CH_2$	π-Alkyl
		$-CH_2$	π-Alkyl
	TRP1369	Ring (Cyclopentyl)	π-Alkyl
		Ring (Cyclohexyl)	π-Alkyl
	ASP1526	-O<u>H</u>	Conventional H-bond (2.82 Å)
	PHE1559	$-CH_2$	π-Alkyl
		$-CH_2$	π-Alkyl
	PHE1560	$-CH_2$	π-Alkyl
3	TYR1251	Phenyl	π-π T-shaped
		$-CH_2$	π-Alkyl
	TRP1355	$-CH_2$	π-Alkyl
		$-CH_2$	π-Alkyl
	TRP1369	$-CH_2$	π-Alkyl
	LYS1460	-C=<u>O</u>	Conventional H-bond (2.36 Å)
		-C=<u>O</u>	Conventional H-bond (2.55 Å)
	ARG1510	-O (Methylenedioxyl)	Conventional H-bond (2.75 Å)
	PHE1559	Phenyl	π-π T-shaped

	PHE1560	Ring (Cyclohexyl)	π-Alkyl
	HIS1584	-O (Methylenedioxyl)	Conventional H-bond (2.79 Å)
Acarbose (Docking control)	ASP1157	-NH_2	Attractive charge
		-OH	Conventional H-bond (1.97 Å)
	GLN1158	-OH	Conventional H-bond (3.04 Å)
	PRO1159	-OH	Conventional H-bond (2.60 Å)
	ASP1279	-OH	Conventional H-bond (2.95 Å)
		-CH_2	Carbon H-bond
	TRP1355	-OH	Conventional H-bond (3.05 Å)
	LYS1460	-O	Conventional H-bond (2.42 Å)
	ASP1562	-NH_2	Attractive charge, salt bridge
		-NH_2	Attractive charge, salt bridge
	HIS1584	-OH	Conventional H-bond (2.49 Å)
		-OH	Conventional H-bond (2.36 Å)

Ligands:α-glucosidase complex

(a) Compound 1

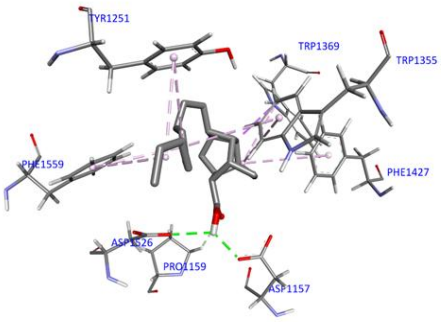

(b) Compound 2

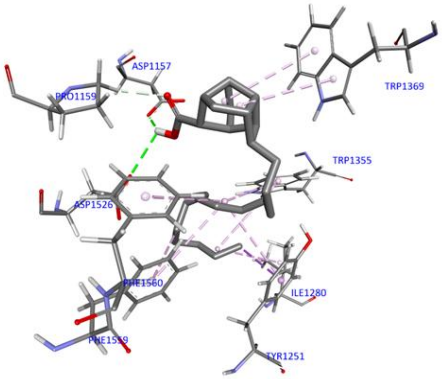

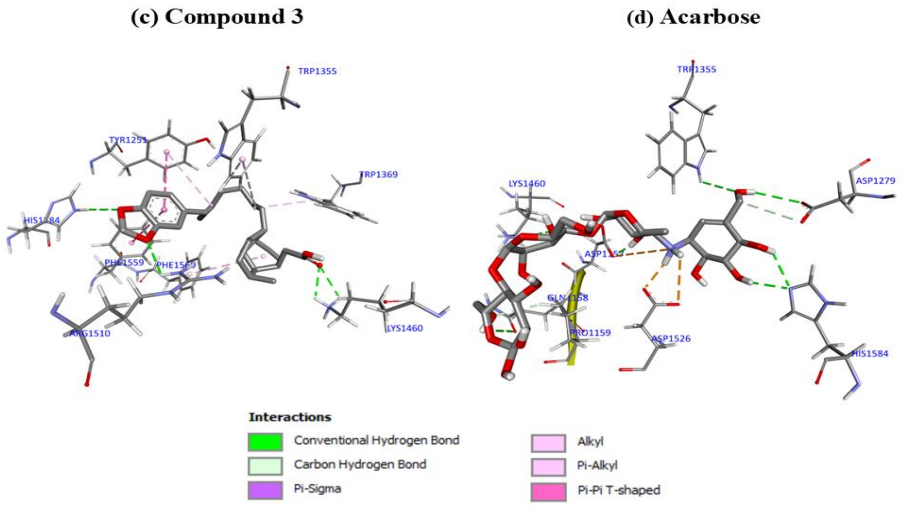

Figure 5. The three-dimensional binding modes of compounds **1**-**3** and acarbose are presented at the active site of α-glucosidase (3TOP).

CONCLUSION

In this research, the phytochemical studies of ethyl acetate crude extracts of *B. lumutensis* yielded three new compounds were isolated; lumutensic acid A (**1**), lumutensic acid B (**2**) and lumutensic acid C (**3**). The molecular docking study revealed that all three isolated compounds exhibited potential inhibitory effects on the hyperglycemic enzymes α-amylase and α-glucosidase, with compound **3** showing the most promising results. Compound **3** had the highest binding affinity and stability for both enzymes, with strong hydrogen bonding and hydrophobic interactions contributing to its superior inhibitory potential. In the α-amylase docking, compound **3** demonstrated the most stable binding (ΔG of -9.070 kcal/mol), forming key interactions with active site residues like ASP300, TRP58, and LEU165. Similarly, for α-glucosidase, compound **3** showed the highest binding energy (ΔG of -9.275 kcal/mol), with multiple hydrogen bonds and hydrophobic interactions involving residues such as LYS1460, ARG1510, and HIS1584, outperforming the control drug acarbose. Compounds **1** and **2** also displayed favorable interactions but with lower binding energies, indicating reduced inhibitory potency. Overall, compound **3** emerges as a strong candidate for further development as a therapeutic agent for managing postprandial hyperglycemia in diabetes.

AUTHORS' CONTRIBUTIONS

Conceptualization: M.N.A.; Methodology: N.A.S. and M.S.A.G.; Investigation: N.A.S. and M.S.A.G.; Formal analysis: N.A.S; M.S.A.G.; M.A.N.; D.S. and U.S.; Data curration: N.A.S; M.S.A.G.; D.S. and U.S.; Validation: M.N.A.; M.A.N.; M.T.C.O. and C.A.; Resources: M.N.A.; M.L.; A.Z. and K.A.; Visualization: N.A.S.; M.S.A.G. and M.N.A.; Writing-original draf preparation: N.A.S.; M.S.A.G. and M.N.A; Writing-review and editting: M.N.A.; Supervision: M.N.A. and M.T.C.O; Project administration: M.N.A. Funding acquisition: M.N.A. All authors have read and agreed to the published version of the manuscript.

ACKNOWLEDGEMENTS

Special thanks to Universiti Sains Malaysia for Internationalisation Incentive Scheme (I^2S) provided (R502-KR-ARP004-00AUPRM003-K134). This research was financially funded through Ministry of Higher Education FRGS FRGS/1/2023/STG04/USM/02/3 and USM RUI grant R502-KR-ARU001-0008012310-K134. This research was conducted within the frame of the collaboration between USM-CNRS (MoU) and auspices of CNRS-UM; Associated International Laboratory (LIA) under FM-NatProLab.

SUPPORTING INFORMATION

Supporting information accompanies this paper on

REFERENCES

Abu Bakar M H, Lee P Y, Azmi M N, Lotfiamir N S, Mohamad M S F, Nor Shahril N S, Shariff K A, Ya'akob H, Awang K, and Litaudon M. (2020). *In vitro* anti-hyperglycemic, antioxidant activities and intestinal glucose uptake evaluation of *Endiandra kingiana* extracts. *Biocatalysis and Agricultural Biotechnology*, 25, 101594.

Apel C, Gény C, Dumontet V, Birlirakis N, Roussi F, Pham V C, Thi Mai H D, Nguyen A H, Chau V M, and Litaudon M. (2014). Endiandric acid analogues from *Beilschmiedia ferruginea* as dual inhibitors of Bcl-xL/Bak and Mcl-1/Bid interactions. *Journal of Natural Products*, 77(6), 1430-1437.

Azmi M N, Gény C, Leverrier A, Litaudon M, Dumontet V, Birlirakis N, Guéritte F, Leong K H, Abd. Halim S N, Mohamad K, and Awang K. (2014). Kingianic acids A–G, endiandric acid analogues from *Endiandra kingiana*. *Molecules*, 19, 1732-1747.

Azmi M N, Péresse T, Remeur C, Chan G, Roussi F, Litaudon M, and Awang K. (2016). Kingianins O–Q: Pentacyclic polyketides from *Endiandra kingiana* as inhibitor of Mcl-1/Bid interaction. Fitoterapia, 109, 190-195.

Azmi M N, Saad N A, Abu Bakar M H, Che Omar M T, Aziz A N, A. Wahab H, Siddiq S, Choudhary M I, Litaudon M, and Awang K. (2021). Cyclic polyketides with α-glucosidase inhibitory activity from *Endiandra kingiana* Gamble and molecular docking study. Records of Natural Products, 15(5), 414-419.

Basir N H, Ramle A Q, Ng M P, Tan C H, Tiekink E R, Sim K S, Basirun W J, and Khairuddean M. (2024). Discovery of indoleninyl-pyrazolo [3,4-b] pyridines as potent chemotherapeutic agents against colorectal cancer cells. *Bioorganic Chemistry*, 146, 1-14.

Bell E W, and Zhang Y. (2019). DockRMSD: An open-source tool for atom mapping and RMSD calculation of symmetric molecules through graph isomorphism. *Journal of Cheminformatics*, 11, 1-9.

Burkill I. (1966). A dictionary of the economic products of the Malay Peninsula. A Dictionary of the Economic Products of the Malay Peninsula. 2(2), 2444 – 2460.

Eberhardt J, Santos-Martins D, Tillack A F, and Forli S. (2021). AutoDock Vina 1.2.0: New docking methods, expanded force field, and python bindings. *Journal of Chemical Information and Modeling*, 61(8), 3891-3898.

Iwu M M. (1993). *Handbook of African medicinal plants* (Second Ed., Vol. 54). CRC Press Inc, Maryland.

Lenta B, Chouna J, Nkeng-Efouet P, and Sewald N. (2015). Endiandric acid derivatives and other constituents of plants from the genera *Beilschmiedia* and *Endiandra* (Lauraceae). *Biomolecules*, *5*(2), 910 – 942

Mahdi B, Azmi M N, Phongphane L, Abd Ghani M S, Bakar M H A, Omar M T C, Mikhaylov A A, and Supratman U. (2024a). Synthesis of *ortho*-carboxamidostilbene analogues and their antidiabetic activity through *in vitro* and *in silico* approaches. *Organic Communications*, 17(1), 8-22.

Mahdi B, Bakar M H A, Omar M T C, Zahari A, Ibrahim M M, Mikhaylov A A, and Azmi M N. (2024b). Synthesis of *para*-carboxamidostilbene derivatives as antihyperglycemia agents and their *in silico* ADMET and molecular docking studies. *ChemistrySelect*, 9(38), e202402433

Maurus R, Begum A, Williams L K, Fredriksen J R, Zhang R, Withers S G, and Brayer, G. D. (2008). Alternative catalytic anions differentially modulate human α-amylase activity and specificity. *Biochemistry*, 47(11), 3332-3344.

Mohamad N, Phua Y H, Bakar M H A, Omar M T C, Wahab H A, Supratman U, Awang K, and Azmi M N. (2021). Synthesis, biological evaluation of ortho-carboxamidostilbenes as potential inhibitors of hyperglycemic enzymes, and molecular docking study. *Journal of Molecular Structure*, 1245, 1-12.

Nishida S. (1999). Revision of *Beilschmiedia* (Lauraceae) in the Neotropics. Annals of the Missouri Botanical Garden, 86(3), 657 – 701.

Pettersen E F, Goddard T D, Huang C C, Couch G S, Greenblatt D M, Meng E C, and Ferrin T E. (2004). UCSF Chimera-A visualization system for exploratory research and analysis. *Journal of Computational Chemistry*, 25(13), 1605-1612.

Phongphane L, Radzuan S N M, Bakar M H A, Omar M T C, Supratman U, Harneti D, A Wahab H, and Azmi M N. (2023). Synthesis, biological evaluation, and molecular modelling of novel quinoxaline-isoxazole hybrid as anti-hyperglycemic. *Computational Biology and Chemistry*, 106, 1-12.

Radzuan S N M, Phongphane L, Bakar M H A, Omar M T C, Shahril N S N, Supratman U, Harneti D, A Wahab H, and Azmi M N. (2024). Synthesis, biological activities, and evaluation molecular docking-dynamics studies of new phenylisoxazole quinoxalin-2-amine hybrids as potential α-amylase and α-glucosidase inhibitors. *RSC Advances*, 14(11), 7684-7698.

Ren L, Qin X, Cao X, Wang L, Bai F, Bai G, and Shen Y. (2011). Structural insight into substrate specificity of human intestinal maltase-glucoamylase. *Protein & Cell*, 2, 827-836.

Saad N A, Azmi M N, and Jumaryatno P. (2022). Mini review on cyclic polyketides from *Beilschmiedia* and *Endiandra* species (Lauraceae): Chemical structures, biological activities and biosynthesis. Malaysian Journal of Chemistry, 24(4), 173-189.

Saad N A, Mohammad S, Bakar M H A, Omar M T C, Litaudon M, Awang K, and Azmi M N. (2022). Anti-hyperglycemic activities, molecular docking and structure-activity relationships (SARs) studies of endiandric acids and kingianins from *Endiandra kingiana*. *Journal of the Brazilian Chemical Society*, 33, 1017-1027.

Şahin İ., Çeşme M, Özgeriş F B, and Tümer F. (2023). Triazole based novel molecules as potential therapeutic agents: Synthesis, characterization, biological evaluation, in-silico ADME profiling and molecular docking studies. *Chemico-Biological Interactions*, 370, 1-13.

Tay Y N, Abu Bakar M H, Azmi M N, Saad N A, Awang K, Litaudon M, and Kassim M A. (2020). Inhibition of carbohydrate hydrolysing enzymes, antioxidant activity and polyphenolic

content of Beilschmiedia species extracts. IOP Conference Series: Materials Science and Engineering, 716, 012007.

Trott O, and Olson A J. (2010). AutoDock Vina: Improving the speed and accuracy of docking with a new scoring function, efficient optimization, and multithreading. *Journal of Computational Chemistry*, 31(2), 455-461.

Zheng L, Meng J, Jiang K, Lan H, Wang Z, Lin M, Li W, Wei Y, and Mu Y. (2022). Improving protein–ligand docking and screening accuracies by incorporating a scoring function correction term. *Briefings in Bioinformatics*, 23(3), 1-15.